

Gaia-EDR3 Parallax Distances to the Great Carina Nebula and its Star Clusters (Trumpler 14, 15, 16)

J. Michael Shull, Jeremy Darling, and Charles Danforth
Department of Astrophysical and Planetary Sciences and CASA
University of Colorado, 389-UCB, Boulder, CO 80309

michael.shull@colorado.edu, jeremy.darling@colorado.edu, charlesdanforth@gmail.com

ABSTRACT

Using offset-corrected Gaia-EDR3 parallax measurements and spectrophotometric methods, we have determined distances for 69 massive stars in the Carina OB1 association and associated clusters: Trumpler 16 (21 stars), Trumpler 14 (20 stars), Trumpler 15 (3 stars), Bochum 11 (5 stars), and South Pillars region (20 stars). Past distance estimates to the Carina Nebula range from 2.2 to 3.6 kpc, with uncertainties arising from photometry and anomalous dust extinction. The EDR3 parallax solutions show considerable improvement over DR2, with typical errors $\sigma_\varpi/\varpi \approx 3\text{--}5\%$. The O-type stars in the Great Carina Nebula lie at essentially the same distance (2.35 ± 0.08 kpc), quoting mean and rms variance. The clusters have distances of 2.32 ± 0.12 kpc (Tr16), 2.37 ± 0.15 kpc (Tr 14), 2.36 ± 0.09 kpc (Tr 15), and 2.33 ± 0.12 kpc (Bochum 11) in good agreement with the η Car distance of around 2.3 kpc. O-star proper motions suggest internal (3D) velocity dispersions ~ 4 km s⁻¹ for Tr 14 and Tr 16. Reliable distances allow estimates of cluster sizes, stellar dynamics, luminosities, and fluxes of photoionizing radiation incident on photodissociation regions in the region. We estimate that Tr 14 and Tr 16 have half-mass radii $r_h = 1.5 - 1.8$ pc, stellar crossing times $t_{cr} = r_h/v_m \approx 0.7 - 0.8$ Myr, and two-body relaxation times $t_{rh} \approx 40 - 80$ Myr. The underlying velocity dispersion for Tr 14, if a bound cluster, would be $v_m \approx 2.1_{-0.4}^{+0.7}$ km s⁻¹ for $N = 7600_{-2600}^{+5800}$ stars. With the higher dispersions of the O-stars, inward drift would occur slowly, on times scales of 3–6 Myr.

1. Introduction

Spanning several square degrees in the Southern sky ($\ell \approx 287^\circ$, $b \approx -0.6^\circ$), the Great Carina Nebula (NGC 3372) and its associated molecular clouds and star clusters are widely investigated as active sites of massive star formation in the Galaxy (Walborn et al. 2012; Smith & Brooks 2008). The O-type stars in the Carina OB1 association (Walborn 1973a; Humphreys 1978; Smith 2006b) are contributors to ionizing radiation, stellar wind mass loss, and other feedback to molecular clouds and the interstellar medium. The Carina region is frequently considered a laboratory for studying the birth and evolution of the most massive stars (Turner & Moffat 1980; DeGioia-Eastwood et al. 2001; Tapia et al. 2003; Hur et al. 2012), including prototypes of updated classifications for the O3 stars (Walborn 1971, 1982a) and O2 stars (Walborn et al. 2002). The Carina Nebula and surrounding molecular clouds are host to a number of star clusters, including Trumpler 14 (Tr 14), Trumpler 15 (Tr 15), Trumpler 16 (Tr 16), Collinder 228 (Col 228), Bochum 11 (Bo 11), and the Treasure Chest Nebula. Illustrative maps of these clusters are shown in papers by Alexander et al. (2016), Kiminki & Smith (2018), Povich et al. (2019), and Smith et al. (2005). The Carina stellar populations are dominated by Tr 14 and Tr 16 together with Tr 15, a less rich cluster with lower extinction. Tr 16 is best known for the presence of η Carinae, a massive, variable star that underwent episodes of brightening

and eruptive mass loss from 1838–1858 (Humphreys & Davidson 1984; Davidson & Humphreys 1997, 2012) after beginning its life with initial mass $\sim 150 M_{\odot}$.

Despite its fundamental importance for stellar astronomy, the Carina Nebula continues to have disparate and controversial values for the distances and ages of its cluster components. Early distance estimates include values of 2.5 kpc (Faulkner 1963), 2.7 kpc (Sher 1965), and 2.8 kpc (Feinstein 1963). More recent estimates cover a wider range from 2–4 kpc (distance moduli $m_V - M_V = 11.5 - 13.0$) with some suggestions that Tr 14 and Tr 16 lie at different distances (Walborn 1973a; Humphreys 1978; Morrell et al. 1988). More accurate estimates of around 2.3 kpc were obtained from geometric methods involving proper motions and Doppler velocities of expanding filaments in the η Car Homunculus. Previous estimates for η Car include 2.2 ± 0.2 kpc (Allen & Hillier 1993), 2.3 ± 0.3 kpc (Meaburn 1999), 2.25 ± 0.18 kpc (Davidson et al. 2001), and 2.35 ± 0.05 kpc (Smith 2006a).

Studies of the Carina OB stars are further complicated because lines of sight in this direction look down the Carina-Sagittarius spiral arm in a complex of dark clouds and bright nebulosity. **Table 1** provides a historical summary of distance estimates for the two main clusters, Tr 14 and Tr 16. Walborn (1973a) placed Tr 14 more distant than Tr 16, but later suggested that they had a common distance of 2.8 kpc (Walborn 1982b, 1995). These differences were primarily the result of uncertainties in the reddening corrections necessary for accurate spectrophotometric distances¹. Large relative distances between Tr 14 and Tr 16 are unlikely, given the association of bright O stars and surrounding nebulosity. Smith (2006b) suggested that Tr 14 might be slightly behind Tr 16, because dark silhouetted objects in the foreground of Tr 14 point toward η Car and Tr 16 (Smith et al. 2003).

The goal of this paper is to obtain more accurate parallax distance estimates for OB stars in the Carina Nebula clusters, using values from the Third (early) Gaia Data Release (EDR3) of the astrometric mission (Gaia Collaboration 2020). This project extends our previous study (Shull & Danforth 2019) of parallax and photometric distances for 139 OB stars. That project used Gaia-DR2 parallaxes and benefited from updated spectral types (SpTs) and visual/near-IR photometry provided by the Galactic O-Star Spectroscopic Survey (GOSS) in papers by Sota et al. (2014; S14) and Maíz Apellániz & Barbá (2018; MAB18). With the longer time interval of observations, the EDR3 parallax solutions show considerable improvement over DR2, as gauged by the parallax-to-error ratio (ϖ/σ_{ϖ}) tabulated in the Gaia archive². In Section 2 we describe our methods for deriving parallax distances, using EDR3 data together with parallax offsets (Lindgren et al. 2020a,b). We compare these distances to spectrophotometric distances derived from GOSS data, when available, with occasional corrections for binary or multiple systems. We present our distance measurements for 69 OB-type stars in the Carina OB1 association and its clusters: Tr 16 (21 stars), Tr 14 (20 stars), Tr 15 (3 stars), Bochum 11 (5 stars), and the South Pillars region (20 stars) around Collinder 228 and Treasure Chest. Our primary result is that, within errors of parallax measurement, the O-type stars in Car OB1 are at essentially the same distance, 2.3–2.5 kpc, in agreement with the η Car distance of 2.35 ± 0.05 kpc (Smith 2006a). Section 3 summarizes our results and their implications for cluster dynamics, stellar absolute magnitudes, and local fluxes of photoionizing radiation incident on molecular gas in the Carina Nebula.

¹Considerable evidence shows that the interstellar dust extinction is anomalous and variable within the Carina region (Feinstein et al. 1973; Thé et al. 1980; Tapia et al. 1988; Smith 2002; Carraro et al. 2004). Ratios of total-to-selective extinction vary from $R_V \approx 3.0 - 3.5$ in Tr 15 and Tr 16 up to $R_V = 3.8 - 4.8$ in Tr 14. These variations are confirmed by extinction measurements from visual and near-infrared photometry (Maíz Apellániz & Barbá 2018) who tabulated values of visual extinction A_{V_j} and the corrected magnitudes, $V_{J,0} \equiv V_J - A_{V_j}$ needed to find the distance modulus, $DM = V_{J,0} - M_V$.

²<https://gea.esac.esa.int/archive>

2. Methods and Measurements

This paper derives both parallax distances and spectrophotometric distances to OB-type stars in the Carina OB1 association. We follow the procedures of our recent OB-star distance survey (Shull & Danforth 2019), using updated parallaxes from Gaia EDR3 and spectrophotometric distances based on photometry and updated SpTs from GOSS. Our sample contains 69 OB stars, with 61 from GOSS. Eight non-GOSS stars were added to increase the samples for Tr 14, Tr 15, and Treasure Chest. Past analyses of Gaia-DR2 data (Lindegren et al. 2018; Arenou et al. 2018; Brown et al. 2018) found systematic fluctuations in parallaxes relative to the reference frame of distant quasars. These offsets appear to be greater toward bright stars (Gaia $G < 12$) and they depend on stellar color and location on the sky. In our previous distance survey, we applied a uniform offset of 0.03 mas to DR2 parallaxes, the recommended DR2 mean (Lindegren et al. 2018). With the new EDR3 data, we computed parallax offsets, ϖ_Z (in mas) from the algorithm produced by the Gaia team (Lindegren et al. 2020b). Most offsets were based on Gaia 5-parameter solutions, with only three stars having 6-parameter solutions (CPD -59° 2591, CPD -59° 2626, HD 93161B). Although the formal Gaia offsets are negative, we follow a convention of quoting positive values in the text and tables. These offsets are added to the EDR3 parallax (ϖ) to find the corrected distance, $D_{\text{EDR3}} = [\varpi + \varpi_Z]^{-1}$. Most stars in Tr 14, Tr 15, and Tr 16 had (EDR3) offsets of 0.011–0.017 mas, with only two as large as 0.025–0.026 mas. The five stars in Bochum 11 had offsets of 0.012–0.013 mas, and most of the 20 stars in the South Pillars region had offsets of 0.011–0.013 mas. One star near the Treasure Chest (CPD -59° 2661) had a larger offset of 0.026 mas.

Table 2 lists EDR3 parallaxes and proper motions with errors from the Gaia archive, together with the parallax offsets found from the Gaia algorithm. The stars are arranged into five groups: Tr 16, Tr 14, Tr 15, Bochum 11, and Other Stars (South Pillars region near Coll 228 and Treasure Chest Nebula). The formal Gaia-EDR3 errors on their parallax solutions listed in Table 2 are typically 3% to 5%, corresponding to $\varpi/\sigma_\varpi = 20 - 30$. There may also be systematic uncertainties in the parallax zero-point offset (Zinn 2021) and problems with parallax solutions in close binaries. Because the relative errors are small, we employed no special procedures to deal with distance bias from parallax inversion. The range of distances ($\pm 1\sigma$) extends from $D_{\text{min}} \equiv [\varpi + \sigma_\varpi]^{-1}$ to $D_{\text{max}} \equiv [\varpi - \sigma_\varpi]^{-1}$ around our tabulated distance of $D_{\text{EDR3}} = \varpi^{-1}$. We averaged the distances toward stars in several Carina Nebula clusters. These mean distances and rms variances are shown in boldface at the end of each grouping.

Table 2 also lists spectrophotometric distances for 69 OB stars in the Car OB1 association, derived by comparing the star’s extinction-corrected magnitude to an absolute magnitude, M_V , based on its SpT and luminosity class. The absolute magnitudes were taken from Table 11 of Bowen et al. (2008), based primarily on calculations by Vacca et al. (1996). As we will show below, this absolute magnitude scale may need to be revised, although the corrections remain poorly determined in this small sample. For most stars (61 out of 69) we relied on GOSS spectral classifications (S14) and photometry (MAB18). From these, we used the extinction-corrected magnitude, $V_{J,0} = V_J - A_{V_J}$ to find the distance, $D_{\text{phot}} = (10 \text{ pc})10^{(V_{J,0} - M_V)/5}$. For the eight other (non-GOSS) stars (HD 93190, HD 303304, Tr 14-3, Tr 14-4, Tr 14-5, Tr 14-6, Tr 14-27, CPD -59° 2661) we relied on photometry from sources in the literature (Hur et al. 2012; Gagné et al. 2011; Alexander et al. 2016; Zacharias et al. 2013). To derive the spectrophotometric distances, we corrected the V magnitudes for extinction by $A_V = R_V E(B - V)$, taking $R_V = 3.1$ for two stars in Tr 15 and $R_V = 4.0$ for five stars in Tr 14.

Figure 1 shows the individual distances for stars in Tr 14, Tr 15, Tr 16, Bo11, and the South Pillars region, plotted vs. the significance level ($S/N \equiv \varpi/\sigma_\varpi$) of the Gaia-EDR3 parallax measurements. Values

of S/N range from 6.8 to 34.9, with means of 19.9 (Tr 16), 25.6 (Tr 15), 23.8 (Tr 14), and 26.2 (Bo 11). We omitted six stars from the Gaia statistical sample, owing to uncertain measurements or missing data: two stars in Tr 16 (CPD -59° 2635 and CPD -59° 2636); two stars in Tr 14 (HD 93161A and Tr 14-5); and two stars in Coll 228 (HD 93146A and HD 93206A). From the D_{phot} sample, we omitted three stars: HD 93162 (WR binary in Tr 16), Tr 14-5, and HD 93146B because of uncertain data. Table 2 lists the mean distances and rms variances of 2.32 ± 0.12 kpc (19 stars in Tr 16); 2.37 ± 0.15 kpc (18 stars in Tr 14); 2.36 ± 0.09 kpc (3 stars in Tr 15); 2.33 ± 0.12 kpc (5 stars in Bochum 11); and 2.45 ± 0.18 kpc (Other Stars group). The two stars near the Treasure Chest are at 2.35 ± 0.08 kpc and 2.41 ± 0.08 kpc. The distance variances for stars in these clusters are 4–5%, and weighting by the individual parallax errors gives similar results. A few stars in our sample could be non-members, and others may have uncertain distances owing to close-binary influence on the parallax solutions. If we consider only the nine stars with SpTs of O5 and earlier, presumed to be the youngest and least dispersed population, we find distances of 2.32 ± 0.08 kpc (five stars in Tr 16), 2.36 ± 0.06 kpc (three stars in Tr 14), and 2.45 ± 0.11 kpc (one star in Tr 15). Taken as a single ensemble, these nine massive O-type stars have a mean distance of 2.35 ± 0.08 kpc (rms variance).

The spectrophotometric distances are more uncertain, with a broader dispersion than in EDR3 parallax. The mean values are larger than the EDR3 distances by 10% (Tr 16), 14% (Tr 14), 12% (Bo 11), and 12% (South Pillars). Better agreement is found using M_V values from Martin et al. (2005). For main-sequence O-type stars, the values in Martins et al. (2005) are typically lower by $\Delta M_V \approx 0.22 - 0.28$ mag (stars are 11–14% closer in distance) compared to M_V in Vacca et al. (1996) and tabulated in Bowen et al. (2008). Other discrepancies may arise from incorrect SpTs or difficulties in correcting the observed magnitudes of spectroscopic binaries. Some previous Carina studies used uncertain corrections for anomalous extinction and variations in R_V . These corrections should be more reliable for the 61 O-type stars drawn from the GOSS sample, where the visual extinction A_{V_j} was derived (MAB18) by modeling the visible/near-IR photometry. For the eight non-GOSS stars, larger uncertainties exist in photometry and SpTs. These issues are discussed further in the Appendix for individual stars.

Formal errors on spectrophotometric distances arise from both photometry and the assumed absolute magnitude (and SpT). The GOSS photometry (MAB18) provided values of visual extinction A_{V_j} and extinction-corrected visual magnitude $V_{J,0} \equiv V_j - A_{V_j}$. The photometric distance is

$$D_{\text{phot}} \equiv (10 \text{ pc})10^{(V_{J,0} - M_V)/5} = (10 \text{ pc}) \exp[(\ln 10/5)(V_{J,0} - M_V)]. \quad (1)$$

Taking partial derivatives of D_{phot} with respect to the two independent variables, $V_{J,0}$ and M_V , we find the propagated distance error,

$$\frac{\sigma_D}{D} = \left(\frac{\ln 10}{5} \right) \left[\sigma_{V_{J,0}}^2 + \sigma_{M_V}^2 \right]^{1/2}. \quad (2)$$

The typical GOSS errors on $V_{J,0}$ are $\sigma_{V_j} = 0.02 - 0.03$, while those on M_V could be as large as $\sigma_{M_V} = 0.15$, corresponding to a half-step in SpT (e.g., O5 V to O5.5 V or O8 V to O8.5 V). For these errors, we find statistical errors on photometric distance of 7% ($0.16 - 0.17$ kpc at $D = 2.3 - 2.4$ kpc).

Figure 2 shows the relation between parallax distance and photometric distances, D_{EDR3} vs. D_{phot} . One immediately sees wide variations in their ratio, emphasizing the unreliability of photometric distances in the Carina Nebula. As noted in previous studies, the Carina region exhibits anomalous extinction, with a range of values of $E(B - V)$ and R_V . The SpTs and absolute magnitude scales may also need recalibration for the massive stars. **Table 3** compares spectrophotometric distances calculated with the two scales. For many stars, the Martins et al. (2005) values provide better agreement with EDR3 distances. The remaining anomalies could be reconciled with studies of more stars in other OB associations.

3. Implications of Distances

The controversy over the disparate distances (d) to Tr 14, Tr 15, and Tr 16 appears to be settled. Within the errors of parallax measurement, the clusters are essentially at the same distance, 2.35 ± 0.08 kpc, in good agreement with the previous distance estimates for η Car: 2.3 ± 0.2 kpc (Allen & Hiller 1993), 2.25 ± 0.18 kpc (Davidson et al. 2001), and 2.35 ± 0.05 kpc (Smith 2006a). These Gaia-EDR3 distances agree with several early recommended values (Thé et al. 1980; Tapia et al. 1988; Walborn 1995), but they differ with subsequent estimates of 2.7–3.6 kpc. The variations are primarily the result of uncertain and variable dust extinction. An accurate distance to the Carina Nebula and its clusters is important for a variety of astrophysical calculations for cluster dynamics, stellar properties, and energy feedback to the surrounding gas. For example, cluster radii scale as $R_c \propto d$, and stellar densities as $n_c \propto d^{-3}$. Cluster masses scale as $M_c \propto d^2$, when inferred from K-band luminosity functions (Ascenso et al. 2007). As we show, the cluster half-mass relaxation time is quite sensitive to distance, $t_{\text{rh}} \propto d^{5/2}$. Thus, a few past estimates of the properties of Tr 14, Tr 16, and the Carina OB1 association may need evaluation.

Smith (2006b) compiled the cumulative energy input of ionizing photon luminosities, stellar mass-loss rates, and mechanical energy production for Carina. At an assumed distance of 2.3 kpc for 65 O-type stars and three Wolf-Rayet stars, he found production rates of $Q_{\text{H}} \approx 10^{51} \text{ s}^{-1}$ of ionizing (Lyman continuum) photons and $L_{\text{w}} \approx 3 \times 10^{38} \text{ erg s}^{-1}$ of stellar-wind mechanical energy. Because his adopted distance is similar to our value, these estimates should be reasonably accurate, subject to recent updates of effective temperatures and Lyman-continuum production rates from non-LTE, line-blanketed model atmospheres (Pauldrach et al. 2001; Puls et al. 2005; Lanz & Hubeny 2007) and evolutionary tracks for stars with winds and rotation (Ekström et al. 2012; Georgy et al. 2013). These effects, and those of metallicity or initial mass function, can alter Q_{H} by factors of three for stellar populations (Topping & Shull 2015). Binary evolution can also affect the time history of $Q_{\text{H}}(t)$ owing to mass transfer, stellar mergers, and atmosphere tidal stripping (Eldridge et al. 2008; de Mink et al. 2013, 2014).

At a distance of 2.35 kpc and angular scale of 1 arcmin = 0.684 pc, the Carina Nebula has a spatial extent of more than 50 pc across the sky. From the cluster centers and circular extents in Tapia et al. (2013) we find radii of 4.40 arcmin (3.0 pc) for Tr 14 and 5.33 arcmin (3.65 pc) for Tr 16. The Tr 14 and Tr 16 centers are separated by 19.7 arcmin (13.5 pc), and Tr 15 and Tr 14 by 16.5 arcmin (11.3 pc). These sizes allow analysis of the dynamical evolution of the star clusters. Trumpler 14 is one of the youngest structures, with an estimated, but uncertain age of $t_{\text{cl}} \approx 0.5 - 1.0$ Myr (Walborn 1995; Tapia et al. 2003). From a near-infrared survey and Kroupa (2001) initial mass function, Ascenso et al. (2007) estimated a cluster mass $M_c \approx (9000 M_{\odot}) d_{2800}^2$ (they assumed a distance of 2800 pc) with a substantial portion coming from pre-main-sequence (PMS) stars. Using near-infrared multi-conjugate adaptive optics on the VLT, Sana et al. (2010) modeled the spatial distribution of stars within Tr 14 to derive $M_c = (4.3_{-1.5}^{+3.3} \times 10^3 M_{\odot}) d_{2500}^2$ (they assumed a distance of 2500 pc). Rescaling their numbers to $d = (2350 \text{ pc}) d_{2350}$ and assuming a mean stellar mass $m_{\text{f}} \approx 0.5 M_{\odot}$, we find that Tr 14 has mass $M_c = (3.8_{-1.3}^{+2.9} \times 10^3 M_{\odot}) d_{2350}^2$ and $N = (7600_{-2600}^{+5800}) d_{2350}^2$ stars within a half-mass radius of $r_{\text{h}} = (1.5 \text{ pc}) d_{2350}$. We adopt an (rms) velocity dispersion for the underlying cluster stars of $v_{\text{m}} \approx (2.1_{-0.4}^{+0.7} \text{ km s}^{-1}) d_{2350}^{1/2}$, assuming the relation for a bound cluster, $v_{\text{m}}^2 \approx 0.4(GM_c/r_{\text{h}})$, from Spitzer (1987). The average stellar density (at $r \leq r_{\text{h}}$) is $n_{\text{h}} = (3/8\pi)(N/r_{\text{h}}^3) \approx (270_{-95}^{+200} \text{ pc}^{-3}) d_{2350}^{-1}$. From these parameters, we estimate two relevant dynamical times for Tr 14,

$$t_{\text{cr}} = r_{\text{h}}/v_{\text{m}} \approx (0.70_{-0.18}^{+0.16} \text{ Myr}) d_{2350}^{1/2} \quad (3)$$

$$t_{\text{rh}} = \frac{v_{\text{m}}^3}{1.22 n_{\text{h}} (4\pi G^2 m_{\text{f}}^2 \ln \Lambda)} = (58_{-11}^{+19} \text{ Myr}) d_{2350}^{5/2}, \quad (4)$$

for the cluster crossing time and the half-mass relaxation time (Spitzer 1987). We have taken the long-range logarithm, $\ln \Lambda \approx \ln(0.4N) \approx 8$. The scaling with distance follows from $r_h \propto d$, $M_c \propto d^2$, $n_h \propto N/r_h^3 \propto d^{-1}$, and $v_m \propto (GM_c/r_h)^{1/2} \propto d^{1/2}$. The two-body relaxation time of the cluster has the greatest sensitivity to distance, with $t_{rh} \propto (v_m^3/n_h) \propto d^{5/2}$.

Given the young age of Tr 14, most stars have probably undergone only one or two orbits within the cluster. The cluster may have expanded as gas was blown out, and a few stars may have moved to outer portions of the cluster where they could be stripped tidally. Young OB associations are believed to be slowly expanding, with 5–30% of their stars ejected as high-velocity stars (Gies 1987; Hoogerwerf et al. 2000). Since t_{rh} is over 50 times the cluster age, most stars in Tr 14 are unlikely to have experienced significant overall relaxation effects (stellar dynamical escape, core collapse). Those effects occur on timescales of $(2-3)t_{rh}$, as found in multi-mass component models of cluster evolution (Spitzer & Shull 1975). The most massive stars in the cluster could drift inward through dynamical friction (Binney & Tremaine 2008) as discussed by Sana et al. (2010). Inward drift of an O-type star of mass $M_* = (40 M_\odot)M_{40}$ would occur on a time scale

$$t_{df} = \frac{V_*^3}{n_f m_f M_* (4\pi G^2 \ln \Lambda)} \approx (6.2 \text{ Myr}) V_4^3 M_{40}^{-1} . \quad (5)$$

Here, we scaled the massive star velocity V_* to the 3D velocity dispersion, $(4 \text{ km s}^{-1})V_4$, found from O-star proper motions internal to Tr 14 and Tr 16 (see below). Thus, the massive stars ($30 - 80 M_\odot$) in these clusters should have undergone little mass segregation over their 1–3 Myr lifetimes.

The Tr 16 cluster is slightly larger than Tr 14 and slightly more dispersed. Previous surveys (DeGioia-Eastwood et al. 2001; Wolk et al. 2011) suggested that its stellar numbers are similar. From source counts, Wolk et al. (2011) found 1232 X-ray sources, matched to 1187 likely near-IR members, and estimated a PMS population of > 6500 class II-III objects. We conservatively adopt a total $N \approx 8000$. With $r_h \approx 1.8 \text{ pc}$, we estimate $n_f \approx 160 \text{ pc}^{-3}$, $M_c \approx 4000 M_\odot$ (with $m_f = 0.5 M_\odot$), $v_m \approx 2.0 \text{ km s}^{-1}$, $t_{cr} \approx 0.8 \text{ Myr}$, and $t_{rh} \approx 80 \text{ Myr}$. The stellar velocity dispersions of Tr 14 and Tr 16 are still uncertain, with estimates from both radial velocity (RV) surveys and EDR3 proper motions. Young clusters will expand as they blow away their nascent cloud material. The velocity dispersion of the O-type stars may exceed our 2.1 km s^{-1} estimate for the underlying stellar population (including PMS stars) assuming a gravitationally bound system. From a survey of the well-constrained stars in Tr 14, Kiminki & Smith (2018) found a weighted-mean heliocentric $RV = 2.3 \pm 7.4 \text{ km s}^{-1}$, comparable to the value, $2.8 \pm 4.9 \text{ km s}^{-1}$, found by Penny et al. (1993) for six O stars. (The total velocity dispersion would be $\sqrt{3}$ times the 1D value.) They regard their 7.4 km s^{-1} dispersion as an upper limit, since it is larger than dispersions of typical, less massive OB associations.

Table 4 lists the proper motions (PM) for individual stars in Carina OB1, for which the Gaia-reported motions (in the Sun’s frame) are dominated by the RA component. To visualize the internal motions, we transformed PMs to the Carina frame by subtracting the mean values for each cluster. We list values of PM in both the Sun’s frame and the cluster rest frame. At 2.35 kpc distance, a PM of 1 mas yr^{-1} corresponds to transverse velocity 11.14 km s^{-1} on the sky. In Table 2, we found a mean total PM for Tr 14 of $6.944 \pm 0.221 \text{ mas yr}^{-1}$ (Sun’s frame) quoting the rms variance among 20 stars. The PM directional components have mean values $PM_{RA} = -6.944 \pm 0.261 \text{ mas yr}^{-1}$ in right ascension (RA) and $PM_{Dec} = 2.185 \pm 0.366 \text{ mas yr}^{-1}$ in declination (Dec), similar to the proper motions found by Kuhn et al. (2019) from a larger number of lower-mass stars. In the Gaia archive tables, $PM^2 = (PM_{RA})^2 + (PM_{Dec})^2$. Table 4 shows the components in RA and Dec, yielding the total PM amplitude. Its propagated uncertainty was found from errors in the individual RA and Dec measurements (typically $\pm 0.014 - 0.027 \text{ mas yr}^{-1}$) and the uncertainty on the cluster mean PMs. We interpret the internal PM amplitude as the (2D) internal velocity dispersion for each cluster. For an isotropic velocity distribution, the 3D dispersion is higher by a

factor $\sqrt{3/2}$. We derive PM errors for each star from the component errors, σ_{PMRA} and σ_{PMDec} ,

$$\sigma_{\text{PM}}^2 = \left(\frac{\text{PM}_{\text{RA}}}{\text{PM}}\right)^2 \sigma_{\text{PMRA}}^2 + \left(\frac{\text{PM}_{\text{Dec}}}{\text{PM}}\right)^2 \sigma_{\text{PMDec}}^2. \quad (6)$$

An interesting ancillary result from the mean values in Table 4 is that Tr 16 appears to be approaching Tr 14 by $0.351 \text{ mas yr}^{-1}$ in RA and $0.427 \text{ mas yr}^{-1}$ in declination (6 km s^{-1} total motion). These values are larger than statistical errors on the mean component PMs.

The 20 OB stars in Tr 14 have a mean 2D internal dispersion of $\sigma_{\text{PM}} = 0.359 \pm 0.058 \text{ mas yr}^{-1}$. Two stars (HD 93160 and ALS 15207) have high PMs ($0.848 \text{ mas yr}^{-1}$), more than twice the cluster mean and thus candidates for escape. If we omit those two stars from the sample, the mean dispersion drops to $\sigma_{\text{PM}} = 0.304 \pm 0.049 \text{ mas yr}^{-1}$, corresponding to velocity dispersions of 3.4 km s^{-1} (2D) and 4.1 km s^{-1} (3D). The 20 stars in Tr 16 have a mean 2D dispersion $\sigma_{\text{PM}} = 0.311 \pm 0.044 \text{ mas yr}^{-1}$, corresponding to velocity dispersions of 3.5 km s^{-1} (2D) and 4.2 km s^{-1} (3D). Two stars (HD 93205 and HD 303316) have high PMs (0.765 and $0.749 \text{ mas yr}^{-1}$) and are escape candidates. Omitting those two stars from the sample reduces the dispersion to $\sigma_{\text{PM}} = 0.262 \pm 0.013 \text{ mas yr}^{-1}$. The group of five O-type stars in Bochum 11 has the smallest mean dispersion, $\sigma_{\text{PM}} = 0.093 \pm 0.023 \text{ mas yr}^{-1}$, corresponding to a 3D velocity dispersion of 1.3 km s^{-1} . The dispersions for the massive OB-type stars suggest that Tr 14 and Tr 16 may not be in virial equilibrium and in the process of dispersing (Kuhn et al. 2019). Multi-body interactions between binaries and cluster stars could transfer energy to these stars and produce expansion of the cluster.

Although Tr 14 has a core-halo structure (Ascenso et al. 2007), no clear evidence has been found for mass segregation (Sana et al. 2010). Proper motions shows that the massive stars have velocities above the assumed value ($v_{\text{m}} \approx 2 \text{ km s}^{-1}$) from the virial equilibrium relation, $v_{\text{m}}^2 \approx 0.4(GM_{\text{c}}/r_{\text{h}})$, adopted by Spitzer (1987). The OB stars may already be expanding from the cluster, with velocities of $3\text{--}4 \text{ km s}^{-1}$ relative to the low-mass PMS stars that dominate two-body relaxation. Inward drift from dynamical friction likely occurs slowly, over $3\text{--}6 \text{ Myr}$, and it might be counteracted by expansionary processes such as gravitational tides, multi-body interactions of stars, and supernova explosions in binary systems. The latter two processes could produce runaway stars (Blauuw 1961; Gies 1987; Hoogerwerf et al. 2000; Bally & Zinnecker 2005).

4. Summary

An encouraging result of our study is that EDR3 parallaxes show considerable improvement over DR2, yielding reliable distances in most cases. Table 2 lists the error range ($D_{\text{min}}, D_{\text{max}}$) about the mean parallax distances D_{EDR3} . With parallax errors, $\sigma_{\varpi} \approx 0.013\text{--}0.020 \text{ mas}$, most OB stars in our Car OB1 survey have fractional errors, $\sigma_{\varpi}/\varpi \approx 3.5\%$ to 5.0% , smaller than the uncertainties in the spectrophotometric distances. These parallax errors correspond to radial distance uncertainties of $40\text{--}100 \text{ pc}$, comparable to the extent of the Carina Nebula on the sky. The main conclusions and implications of our study are as follows:

1. For the youngest stellar populations (O5 and earlier), we find distances of $2.32 \pm 0.08 \text{ kpc}$ (five stars in Tr 16); $2.36 \pm 0.06 \text{ kpc}$ (three stars in Tr 14); and $2.45 \pm 0.11 \text{ kpc}$ (one star in Tr 15) quoting rms variances. Taken as a single ensemble, these nine stars have a mean distance of $2.35 \pm 0.08 \text{ kpc}$ (rms).
2. The uniformity in parallax distances to Tr 14, Tr 15, Tr 16, Bo 11, and Treasure Chest is consistent with observations of anomalous and variable dust extinction within the Carina Nebula. Comparisons of EDR3 distances to new spectrophotometric parallaxes confirm the high values of $R_V \approx 4$ for Tr 14

compared to Tr 16 and Tr 15. The current survey is consistent with the prescient statement (Walborn 1995) in his review of the Carina Nebula: “If $R(\text{Tr } 14) = R(\text{Tr } 16) + 1$, there would be no need for either a distance or age difference between the two clusters”.

3. An established distance ($d \approx 2.35$ kpc) to the Carina Nebula provides confidence in the previous calibration of stellar luminosities, FUV fluxes, and mass-loss rates (Smith 2006b) based on $d = 2.3$ kpc. With new model atmospheres, these may shift together with new stellar scales of T_{eff} , M_V , and ionizing photon production. These parameters determine the photoevaporation rates of protoplanetary disks and properties of gas pillars and photodissociation regions (Smith & Brooks 2008).
4. With $d = 2.35$ kpc, the cluster two-body relaxation time, $t_{\text{rh}} \propto d^{5/2}$, is reduced significantly from previous values at 2.5–2.8 kpc distances. The star clusters appear dynamically young. With radii of 3–4 pc, Tr 14 and Tr 16 have stellar crossing times 0.7–0.8 Myr and relaxation times $t_{\text{rh}} \approx 40 - 80$ Myr. Proper motions of the O-type stars in Tr 14 and Tr 16 suggest velocity dispersions of 3–4 km s⁻¹. Massive stars could drift inward by dynamical friction on 6 Myr times scales. Thus, mass segregation and inward drift are unlikely to be observable for these dynamically young clusters.
5. We identified stars in Tr 14 (HD 93160 and ALS 15207) and Tr 16 (HD 93205 and HD 303316) with proper motions more than twice the cluster dispersion. These stars could be candidates for escape, produced by multi-body stellar interactions. Although no obvious supernovae have been found in the Carina Nebula, runaway stars from dense cluster cores would travel 20–100 pc over 1 Myr.
6. Most parallax distances in Car OB1 are more accurate than spectrophotometric estimates found from GOSS photometry and SpTs. Mean photometric distances to Tr 14, Tr 16, and Bo 11 are 10–14% larger than Gaia-EDR3 distances. A set of massive stars at a common distance with reliable reddening models (e.g., GOSS) could enable a calibration of absolute magnitudes. For most main-sequence O-stars, the Martins et al. (2008) scale of M_V gives somewhat better agreement with EDR3 distances.

Acknowledgements. We thank Nathan Smith, Roberta Humphreys, John Bally, for helpful discussions about the Carina Nebula and Kris Davidson and Bill Vacca for comments on distance measurements. This work has made use of data from the European Space Agency (ESA) mission Gaia (<https://www.cosmos.esa.int/gaia>), processed by the Gaia Data Processing and Analysis Consortium (DPAC, <https://www.cosmos.esa.int/web/gaia/dpac/consortium>). Funding for the DPAC has been provided by national institutions, in particular the institutions participating in the Gaia Multilateral Agreement.

A. Notes on Individual Stars

CPD -59° 2603. This is a hierarchical triple system, also known as V572 Car, with spectral classification [O7.5 V + B0 V] in Table 7 of S14. An alternate classification of [O7 V + O9.5 V + B0.2 IV] comes from high-resolution spectra (Rauw et al. 2001). From GOSS photometry (MAB18) of the full system, we use $V_{J,0} = 7.17$ and adopt $M_V = -4.75$ (for O7 V) to find $D_{\text{phot}} = 2.42$ kpc. This distance is slightly less than the Gaia-EDR3 value of 2.62 kpc (range 2.48–2.78 kpc).

CPD -59° 2624. Also known as Tr 16-9, this star was incorrectly listed as CPD-59°2634 in the GOSS papers (S14 and MAB18). The SpT is O9.7 IV (S14) for which $M_V = -4.56$ for O9.7 IV (Bowen et al. 2008). We adopt an extinction corrected $V_{J,0} = 7.603 \pm 0.016$ (MAB18) to find $D_{\text{phot}} = 2.71$ kpc. This photometric

distance would decrease to 2.24 kpc if we used the O9.5 V SpT of Nelan et al. (2004) and $M_V = -4.15$. This shorter distance would be in better agreement with the Gaia value, $D_{\text{EDR3}} = 2.26$ kpc (range 1.98–2.64) kpc.

CPD -59° 2635. This is a spectroscopic binary, classified by GOSS (S14) as [O8 V + O9.5 V] with an extinction-corrected magnitude (MAB18) of $V_{J,0} = 6.844 \pm 0.019$ with $A_{V_J} = 2.437 \pm 0.025$. Adopting $M_V = -4.60$ for O8 V (Bowen et al. 2008) we find $D_{\text{phot}} = 2.50$ kpc, after correcting the distance to the two stars with a multiplicative factor $[1 + (L_2/L_1)]^{1/2} = 1.29$ for $L_2/L_1 = 0.661$.

CPD -59° 2636AB. Also known as Tr 16-110, this star had no parallax solution in either DR2 or EDR3 of the Gaia archive. It appears in the GOS survey (S14) as a spectroscopic binary [O8 V + O8 V] with an extinction-corrected magnitude (MAB18) of $V_{J,0} = 6.493 \pm 0.019$ with $A_{V_J} = 2.726 \pm 0.021$. With $(B - V) = 0.34$ and $(B - V)_0 = -0.31$, we find $E(B - V) = 0.65$, consistent with $R_V \approx 4$. Adopting $M_V = -4.60$ for O8 V (Bowen et al. 2008) we find $D_{\text{phot}} = 2.34$ kpc, after correcting the distance to the two O8 V stars with a multiplicative factor $[1 + (L_2/L_1)]^{1/2} = \sqrt{2}$. The lack of a parallax solution may arise because the system is actually quadruple (S14).

HD 93129AB. GOSS (S14) lists both A and B stars as HD 93129AaAb (O2 If*) and HD 93129B [O3.5 V((f))]. GOSS photometry (MAB18) lists an extinction-corrected magnitude $V_{J,0} = 4.825 \pm 0.029$ with $A_{V_J} = 2.199 \pm 0.025$ for the combined system (AaAbB). The AaAb binary was classified by Gruner et al. (2019) as [O2 If* + O3 III(f*)] with $V_{\text{Aa}} = 7.65$, $V_{\text{Ab}} = 8.55$, and $(B - V) = 0.25$. Using $(B - V)_0 = -0.32$, we adopt $E(B - V) = 0.57$ for the system (Aa, Ab, and B) and a combined magnitude $V_{\text{AaAb}} = 7.26$. With a combined $M_V = -6.49$ for Aa+Ab, we find $D_{\text{phot}} = 2.49$ kpc, a distance that we assign to both A and B.

HD 93146AB. This is a multiple system located in the Collinder 228 region. GOSS (S14) tabulates two separate stars, an SB1 spectroscopic binary HD 93146A (O7 Vfz) and HD 93146B (O9.7 IV). GOSS photometry (MAB18) lists extinction-corrected magnitudes, $V_{J,0}(A) = 6.905 \pm 0.027$ with $A_{V_J} = 1.535 \pm 0.029$ and $V_{J,0}(B) = 8.602 \pm 0.027$ with $A_{V_J} = 1.324 \pm 0.046$. Adopting $M_V(A) = -4.90$ (O7 V) and $M_B(B) = -4.56$ (O9.7 IV), we derive photometric distances of 2.30 kpc (A) and 4.29 kpc (B), considerably different from the offset-corrected Gaia-EDR3 parallax distances, 2.93 kpc (A) and 2.47 kpc (B). These discrepancies are puzzling, since A and B are separated by just 6.5'' (Figure 12a of S14). The GOSS magnitude, $V_J = V_{J,0} + A_{V_J} = 9.926 \pm 0.053$ is slightly fainter than $V = 9.864$ (Gagné et al. 2011) whose $(B - V) \approx 0.00$ indicates $E(B - V) \approx 0.31$. This color excess is consistent with the GOSS value, $A_{V_J}/R_V \approx 0.33$. The SpT of HD 93146B may be wrong, leading to an incorrect M_V , although it would need to be early B-type. Alternately, HD 93146B could be a background star.

HD 93161AB. GOSS (S14) tabulates A and B stars separately: an SB2 binary HD 93161A [O7.5 V + O9 V] and HD 93161B (O6.5 IV). However, GOSS photometry (MAB18) lists extinction-corrected magnitudes for the full system (AB) with $V_{J,0} = 5.776 \pm 0.017$ with $A_{V_J} = 2.038 \pm 0.026$. To obtain an absolute magnitude for the AB system, we combine $M_V = -4.75$ (O7.5 V) with $M_V = -4.30$ (O9 V) to obtain $M_V(A) = -5.30$, and then with $M_V(B) = -5.40$ (O6.5 IV) to find $M_V(AB) = -6.10$. This yields a system photometric distance of $D_{\text{phot}} = 2.37$ kpc. Nazé et al. (2015) provided individual photometry and modeling, with $R_V = 3.8$, $V_A = 8.56 \pm 0.02$ and $V_B = 8.60 \pm 0.02$. Color indices $(B - V) = 0.20$ (A) and 0.23 (B) correspond to $E(B - V)$ of 0.52 (A) and 0.55 (B). The combined magnitude is $V_{AB} = 7.83 \pm 0.02$, similar to the GOSS value of 7.81 ± 0.03 (MAB18). With $M_V(A) = -5.21$ for their [O8 V + O9 V] classification and $M_V(B) = -5.40$ for O6.5 IV, we obtain photometric distances of 2.28 kpc (A) and 2.41 kpc (B), adopting their value of $R_V = 3.80$. The Gaia-EDR3 archive lists different parallaxes for component A (0.3399 ± 0.0281 mas) and component B (0.3859 ± 0.0282 mas). After offset corrections, those correspond to EDR3 distances of 2.84 kpc (A) and 2.48 kpc (B). This suggests potential problems with the parallax solution from system multiplicity.

HD 93190. This star appeared in GOSS with an uncertain O9.7:V classification (S14), but no GOSS photometry was found (MAB18). We adopt $B = 9.10 \pm 0.02$ and $V = 8.84 \pm 0.04$ (Zacharias et al. 2013), from which we estimate $E(B - V) = 0.56$ from $(B - V) = 0.26$ and $(B - V)_0 = -0.30$. With $M_V = -4.00$ for this SpT, we find an uncertain spectrophotometric distance of 1.66 kpc, considerably lower than the Gaia-EDR3 value of 2.35 kpc (range 2.25–2.45 kpc). The uncertain SpT makes this an unreliable distance.

HD 93206A. The variable QZ Car is the brightest object in the Collinder 228 cluster and ID#46 in our distance survey (Shull & Danforth 2019). This is a double-line (SB1+SB1) binary (Parkin et al. 2011), consisting of system A (O9.7 Ib + b2 v) and system B (O8 III + o9 v). GOSS gives a combined classification of O9.7 Ib (S14) with $V_{J,0} = 4.206 \pm 0.018$ and $A_{V,J} = 2.106 \pm 0.022$ (MAB18), presumably including all four stars in HD 93206AB. Our photometric distance estimate, $D_{\text{phot}} = 2.23$ kpc, is based on the Aa component (O9.7 Ib) with $V = 6.31$ and $M_V = -6.18$, corrected for the luminosity ratio $L_2/L_1 = 0.535$ of the two brightest stars (O8 III and O9.5 Ib), increasing the distance by a factor $[1 + (L_2/L_1)]^{1/2} = 1.24$.

HD 93222. GOSS (S14) classifies this star as O7 Vfz, and photometry (MAB18) has $V_{J,0} = 6.265 \pm 0.019$ and $A_{V,J} = 1.837 \pm 0.021$. The O7 V classification with $M_V = -4.90$ would yield an unrealistically small spectrophotometric distance of $D_{\text{phot}} = 1.71$ kpc. Instead, as recommended by Shull & Danforth (2019) for this star (ID #47), we adopt O7 IIIf from Markova et al. (2011) and Walborn (1973b) with $M_V = -5.70$, yielding $D_{\text{phot}} = 2.47$ kpc.

HD 303304. This star did not appear in GOSS (S14), and no photometry was found (MAB18). The Simbad website lists an uncertain SpT of O7-8 V and photometry of $B = 10.08 \pm 0.20$ and $V = 9.67 \pm 0.32$ from Alexander et al. (2016). From this, we estimate $E(B - V) \approx 0.73$ from $(B - V) = 0.41$ and $(B - V)_0 = -0.32$. We adopt $M_V = -4.75$, intermediate between -4.90 (O7 V) and -4.60 (O8 V), for a spectrophotometric distance 2.70 kpc, somewhat higher than the Gaia-EDR3 value of 2.28 kpc (range 2.21–2.35 kpc). Because of the uncertain photometry, reddening, and SpT, this is an unreliable distance.

HD 303311. GOSS photometry (MAB18) listed extinction-corrected $V_{J,0} = 7.448 \pm 0.018$ and $A_{V,J} = 1.523 \pm 0.024$, and S14 classify it as O6 V((f))z. With $M_V = -5.20$ (Bowen et al. 2008) we find $D_{\text{phot}} = 3.39$ kpc. Walborn (1982a) classifies the star as O5 V, while Alexander et al. (2016) list it as O8 III((f)), with alternate SpTs of O7 V or O6 V((f))z and a possible spectroscopic binary. The Gaia-EDR3 parallax distance is 2.24 kpc (range 2.17–2.31 kpc). The O8 III classification ($M_V = -5.50$) would lead to a distance of 3.89 kpc. Better agreement between D_{phot} and D_{EDR3} would be found with a later SpT. For example, a main-sequence classification of O8 V with $M_V = -4.60$ would give $D_{\text{phot}} = 2.57$ kpc.

HD 305518. GOSS photometry (MAB18) lists extinction-corrected $V_{J,0} = 7.284 \pm 0.022$ and $A_{V,J} = 2.435 \pm 0.032$, and S14 classify it as O9.7 III. With $M_V = -5.10$ (Bowen et al. 2008) we find $D_{\text{phot}} = 3.00$ kpc, which is considerably larger than $D_{\text{EDR3}} = 2.00$ kpc (range 1.92–2.08 kpc). This star is fairly distant from Tr 16 on the sky and loosely associated with Col 228. If the DR3 parallax is reliable, the star could be in the foreground. It is difficult to decide, given the disparity between the two distances.

HD 305532. This star is located near the Treasure Chest, with an EDR3 distance of 2.41 ± 0.08 kpc. GOSS photometry (MAB18) lists extinction-corrected $V_{J,0} = 7.216 \pm 0.023$ and $A_{V,J} = 2.946 \pm 0.040$, and S14 classify it as O6.5 V((f))z. With $M_V = -5.05$ (Bowen et al. 2008) we find $D_{\text{phot}} = 2.84$ kpc, which is greater than $D_{\text{EDR3}} = 2.41$ kpc (range 2.33–2.49 kpc). The star may be an unresolved SB1 binary (Levato et al. 1990). However, a standard luminosity correction would worsen the discrepancy, increasing the photoelectric distance by a factor $[1 + (L_2/L_1)]^{1/2}$. This suggests that the star may have a fainter M_V than we adopted for its SpT of O6.5 V in GOSS.

CPD –59° 2661. This star is located near the Treasure Chest, with an EDR3 distance of 2.35 ± 0.08 kpc. This star did not appear in GOSS (S14), and no photometry was found (MAB18). Walsh (1984) found a SpT of O9.5 V, and photometry of $B = 11.55 \pm 0.16$ and $V = 11.20 \pm 0.18$ comes from Zacharias et al. (2013). From this, we estimate $E(B - V) \approx 0.66$ from $(B - V) = 0.35$ and $(B - V)_0 = -0.31$, in agreement with $E(B - V) = 0.65 \pm 0.04$ and $R_V = 4.8$ from hydrogen recombination line ratios (Smith et al. 2005). With $M_V = -4.15$ (Bowen et al. 2008), we find $D_{\text{phot}} = 2.79$ kpc, with at least 10% uncertainty from photometry errors. This suggests that the star may have a fainter M_V than we adopted for its SpT of O9.5 V.

Tr 14-3. This star did not appear in GOSS (S14), and no photometry was found (MAB18). Nelan et al. (2004) list a SpT of B0.5 IV-V, originally classified by Morrell et al. (1988). Levato et al. (2000) found that Tr 14-3 is a double-lined spectroscopic binary, with approximate masses of $20 M_\odot$ and $15 M_\odot$. Hur et al. (2012) quoted $B = 11.00$ and $V = 10.73$. With $(B - V) = 0.27$ and $(B - V)_0 = -0.28$, we find $E(B - V) = 0.55$. We adopt $M_V = -3.88$, intermediate between -3.55 (B0.5 V) and -4.20 (B0.5 IV). If $R_V = 4.0$, the spectrophotometric distance would be 3.03 kpc. Instead, we adopt a SpT of B0.5 V, under the assumption that the B stars in Tr14 should still be on the main sequence. We quote an uncertain distance $D_{\text{phot}} = 2.61$ kpc, close to the Gaia-EDR3 distance of 2.42 kpc (range 2.35–2.49 kpc).

Tr 14-4. This star did not appear in GOSS (S14), and no photometry was found (MAB18). Gagné et al. (2011) classified this star as B0 V, and Hur et al. (2012) quoted $B = 11.32$ and $V = 11.04$. With $(B - V) = 0.28$ and $(B - V)_0 = -0.30$, we have $E(B - V) = 0.58$. With $M_V = -4.30$ and $R_V = 4.0$, we find an uncertain $D_{\text{phot}} = 3.27$ kpc, considerably higher than the Gaia-EDR3 distance of 2.62 kpc (range 2.54–2.71 kpc). An incorrect SpT, higher extinction, or $R_V \geq 4.5$ could all account for the difference.

Tr 14-5. This star did not appear in GOSS (S14), and no photometry was found (MAB18). Gagné et al. (2011) classified this star as O9 V, and Hur et al. (2012) quoted $B = 11.63$ and $V = 11.30$. With $(B - V) = 0.33$ and $(B - V)_0 = -0.31$, we find $E(B - V) = 0.64$. With $M_V = -4.30$ and $R_V = 4.0$, we find an uncertain $D_{\text{phot}} = 4.06$ kpc, considerably higher than the Gaia-EDR3 distance of 2.83 kpc (range 2.71–2.96 kpc). An incorrect SpT, higher extinction, or $R_V \geq 4.5$ could all account for the difference.

Tr 14-6. This star did not appear in GOSS (S14) and no photometry was found (MAB18). Gagné et al. (2011) classified this star as B1 V, and Hur et al. (2012) quoted $B = 11.33$ and $V = 11.12$. With $(B - V) = 0.21$ and $(B - V)_0 = -0.26$, we find $E(B - V) = 0.47$. With $M_V = -3.04$ and $R_V = 4.0$, we find an uncertain $D_{\text{phot}} = 2.86$ kpc, higher than the Gaia-EDR3 distance of 2.26 kpc (range 2.18–2.34 kpc).

Tr 14-27. This star did not appear in GOSS (S14), and no photometry was found (MAB18). Alexander et al. (2011) classified this star as B1.5 V, and Hur et al. (2012) quoted $B = 11.54$ and $V = 11.22$. With $(B - V) = 0.32$ and $(B - V)_0 = -0.25$, we estimate $E(B - V) = 0.57$. With $M_V = -4.30$ and $R_V = 4.0$, find $D_{\text{phot}} = 2.09$ kpc, less than the Gaia-EDR3 distance of 2.21 kpc (range 2.15–2.28 kpc).

ALS 15210. This star was classified as O3.5 If* in(S14), but no GOSS photometry was provided (MAB18). Hur et al. (2012) quoted $B = 11.507$ and $V = 10.709 \pm 0.013$. With $(B - V) = 0.80$ and $(B - V)_0 = -0.26$, we estimate $E(B - V) \approx 1.12$. The correction factor $R_V = A_V/E(B - V)$ is likely large but uncertain. We adopt $R_V = 4.5$ and $A_V \approx 5.0$ mag, similar to the GOSS value (MAB18) for the nearby star HD 93162. With $M_V = -6.30$ for O6 Ib (Bowen et al. 2008) we find $D_{\text{phot}} = 2.48$ kpc, similar to the Gaia-EDR3 distance of 2.40 kpc (range 2.32–2.48 kpc). This photometric distance comes with considerable uncertainty owing to the reddening correction.

REFERENCES

- Alexander, M. J., Hanes, R. J., Povich, M. S., & McSwain, M. V. 2016, *AJ*, 152, 190
- Allen, D. A., & Hillier, D. J. 1993, *PASA*, 10, 338
- Arenou, F., Luri, X., Babusiaux, C., et al. 2018, *A&A*, 616, A17
- Ascenso, J., Alves, J., Vicente, S., & M. T. V. T. 2007, *A&A*, 476, 199
- Bally, J., & Zinnecker, H. 2005, *AJ*, 129, 2281
- Binney, J., & Tremaine, S. 2008, *Galactic Dynamics* (Princeton: Princeton University Press)
- Blaauw, A. 1961, *B.A.N.*, 15, 265
- Bowen, D. V., Jenkins, E. B., Tripp, T. M., et al. 2008, *ApJS*, 176, 59
- Brown, A. G. A., Vallenari, A., Prusti, T., et al. 2018, *A&A*, 616, 1
- Carraro, G., Romaniello, M., Ventura, P., & Patat, F. 2004, *A&A*, 418, 525
- Davidson, K., Helmel, G., & Humphreys, R. M. 2018, *RNAAS*, 2, 133 (arXiv:1808.02073)
- Davidson, K., & Humphreys, R. M. 1997, *ARA&A*, 35, 1
- Davidson, K., & Humphreys, R. M. 2012, in *Eta Carinae and the Supernova Imposters*, *ASSL*, Springer Publ., 384, 1
- Davidson, K., Smith, N., Gull, T. R., et al. 2001, *AJ*, 121, 1569
- DeGioia-Eastwood, K., Throop, H., Walker, G., & Cudworth, K. M., 2001, *ApJ*, 549, 578
- de Mink, S. E., Langer, N. E., Izzard, R. G., & Schneider, F. R. N. 2014, *ApJ*, 782, 7
- de Mink, S. E., Sana, H., Langer, N. E., Izzard, R. G., Sana, H., & de Koter, A. 2013, *ApJ*, 764, 166
- Eldridge, J. J., Izzard, R. G., & Tout, C. A. 2008, *MNRAS*, 384, 1109
- Ekström, S., Georgy, C., Eggenberger, P., et al. 2012, *A&A*, 537, A146
- Faulkner, D. J. 1963, *PASP*, 75, 269
- Feinstein, A. 1963, *PASP*, 75, 492
- Feinstein, A., Marraco, H. G., & Muzzio, J. C. 1973, *A&AS*, 12, 331
- Gaia Collaboration, Brown, A. G. A., et al. 2020, *A&A*, in press (arXiv:2012.01533)
- Gagné, M., Fehon, G., Savoy, M. R., et al. 2011, *ApJS*, 194, 5
- Georgy, C., Ekström, S., Meynet, G., et al. 2013, *A&A*, 542, A29
- Gies, D. R. 1987, *ApJS*, 64, 545
- Gruner, D., Hainich, R., Sander, A. A. C., et al. 2019, *A&A*, 621, A63
- Hoogerwerf, R., de Bruijne, J. H. J., & de Zeeuw, P. T. 2000, *ApJ*, 544, L133
- Humphreys, R. M. 1978, *ApJS*, 38, 309
- Humphreys, R. M., & Davidson, K. 1984, *Science*, 223, 243
- Hur, H., Sung, H., & Bessell, M. S. 2012, *AJ*, 143, 41
- Kiminki, M. M., & Smith, N. 2018, *MNRAS*, 477, 2068
- Kroupa, P. 2001, *MNRAS*, 322, 231
- Kuhn, M. A., Hillenbrand, L. A., Sills, A., et al. 2019, *ApJ*, 870, 32

- Lanz, T., & Hubeny, I. 2007, *ApJS*, 169, 83
- Levato, H., & Malaroda, S. 1981, *PASP*, 93, 714
- Levato, H., Malaroda, S., García, B., Morrell, N., & Solivella, G. 1990, *ApJS*, 72, 323
- Levato, H., Malaroda, S., Morrell, N., García, B., & Grosso, M. 2000, *PASP*, 112, 359
- Lindegren, L., Hernández, J., Bombrun, A., et al. 2018, *A&A*, 616, A2
- Lindegren, L., Klioner, S. A., Hernández, J., et al. 2020a, *A&A*, in press (arXiv:2012.03380)
- Lindegren, L., Bastian, U., Biermann, M., et al. 2020b, *A&A*, in press (arXiv:2012.01742)
- Maíz Apellániz, J., & Barbá, R. H. 2018, *A&A*, 613, A9 (MAB18)
- Markova, N., Puls, J., Scuderi, S., Simón-Díaz, S., & Herrero, A. 2011, *A&A*, 530, A11
- Martins, F., Schaerer, D., & Hillier, D. J. 2005, *A&A*, 436, 1049
- Massey, P., & Johnson, J. 1993, *AJ*, 105, 980
- Meaburn, J. 1999, in *Eta Carinae at the Millennium*, ed. J. A. Morse, R. M. Humphreys, & A. Damieli (San Francisco, ASP), *ASP Conf. Ser.*, 179, 89
- Morrell, N., Garcia, B., & Levato, H. 1988, *PASP*, 100, 1431
- Nazé, Y., Antokhin, I. I., Sana, H., Gosset, E., & Rauw, G. 2005, *MNRAS*, 359, 688
- Nelan, E. P., Walborn, N. R., Wallace, D. J., et al. 2004, *AJ*, 128, 323
- Parkin, E. R., Broos, P. S., Townsley, L. K., et al. 2011, *ApJS*, 194, 8
- Pauldrach, A. W. A., Hoffmann, T. L., & Lennon, M. 2001, *A&A*, 275, 161
- Penny, L. R., Gies, D. R., Hartkopf, W. I., Mason, B. D., & Turner, N. H. 1993, *PASP*, 105, 588
- Povich, M. S., Maldonado, J. T., Nunez, E. H., & Robitaille, T. P. 2019, *ApJ*, 881, 37
- Puls, J., Urbaneja, M. A., Venero, R., et al. 2005, *A&A*, 435, 669
- Rauw, G., Nazé, Y., Carrier, F., et al. 2001, *A&A*, 368, 212
- Sana, H., Momany, Y., Gieles, G., et al. 2010, *A&A*, 515, A26
- Sher, D. 1965, *QJRAS*, 6, 299
- Shull, J. M., & Danforth, C. W. 2019, *ApJ*, 882, 180
- Smith, N. 2002, *MNRAS*, 331, 7
- Smith, N. 2006a, *ApJ*, 644, 1151
- Smith, N. 2006b, *MNRAS*, 367, 763
- Smith, N., Bally, J., & Morse, J. A. 2003, *ApJ*, 587, L105
- Smith, N., & Brooks, K. J. 2008, in *Handbook of Star Forming Regions, Vol. II*, ASP Publisher, ed. B. Reipurth, 138 (arXiv:0809.5081)
- Smith, N., Stassun, K. G., & Bally, J. 2005, *AJ*, 129, 888
- Sota, A., Maíz Apellániz, J., Morrell, N. I., et al. 2014, *ApJS*, 211, 10 (S14)
- Spitzer, L., Jr. 1987, *Dynamical Evolution of Globular Clusters* (Princeton: Princeton University Press)
- Spitzer, L., & Shull, J. M. 1975, *ApJ*, 201, 773
- Tapia, M., Roth, M., Marraco, H., & Ruiz, M.-T. 1988, *MNRAS*, 232, 661

- Tapia, M., Roth, M., Vázquez, R. A., & Feinstein, A. 2003, *MNRAS*, 339, 44
- Thé, P. S., & Vleeming, G. 1971, *A&A*, 14, 120
- Thé, P. S., Bakker, R., & Antalova, A. 1980, *A&AS*, 41, 83
- Topping, M. W., & Shull, J. M. 2015, *ApJ*, 800, 97
- Turner, D. G., & Moffat, A. F. J. 1980, *MNRAS*, 192, 283
- Vacca W. D., Garmany, C. D., & Shull, J. M. 1996, *ApJ*, 460, 914
- Vázquez, R. A., Baume, G., Feinstein, A., & Prado, P. 1996, *A&AS*, 116, 75
- Walborn, N. R. 1971, *ApJ*, 167, L31
- Walborn, N. R. 1973a, *ApJ*, 179, 517
- Walborn, N. R. 1973b, *AJ*, 78, 1067
- Walborn, N. R. 1982a, *ApJ*, 254, L15
- Walborn, N. R. 1982b, *AJ*, 87, 1300
- Walborn, N. R. 1995, *Rev. Mex. Astron. Astrofis. Ser. Conf.*, 2, 51
- Walborn, N. R. 2012, in *Eta Carinae and the Supernova Imposters*, *ASSL*, Springer Publ., 384, 25
- Walborn, N. R., Howarth, I. D., Lennon, D. J., et al. 2002, *AJ*, 123, 2754
- Walsh, J. R. 1984, *A&A*, 138, 380
- Wolk, S. J., Broos, P. S., Getman, K. V., et al. 2011, *ApJS*, 194, 12
- Zacharias, N., Finch, C. T., Girard, T. M., et al. 2013, *AJ*, 145, 44
- Zinn, J. C. 2021, *ApJ*, in press (arXiv:2101.07252)

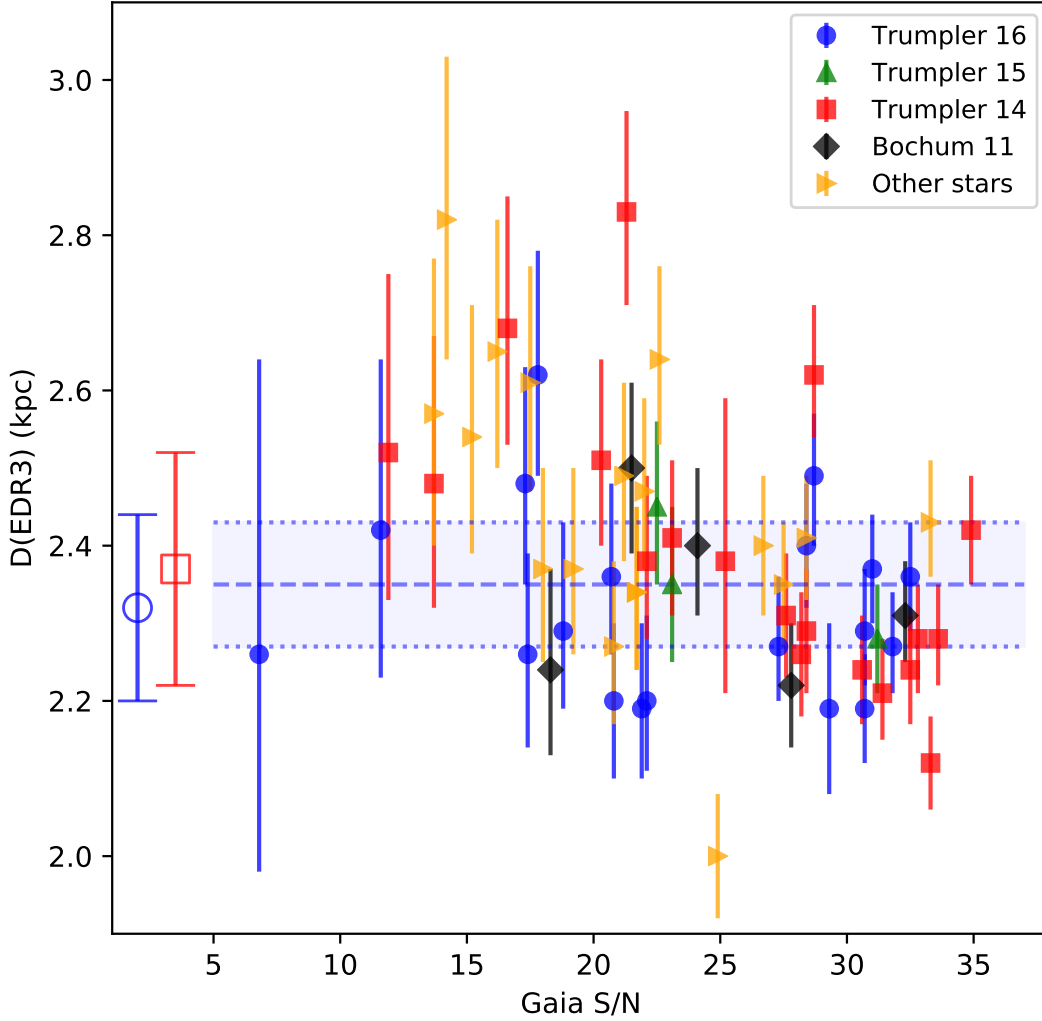


Fig. 1.— Offset-corrected parallax distances from Gaia-EDR3 versus the significance level, $S/N = \varpi/\sigma_\varpi$, of the measurement. We show individual values for 46 OB-type stars in the Carina Nebula, color-coded for four clusters (Tr 16, Tr 15, Tr 14, Bo 11) and other stars around Col 228. The mean distance and (rms) variance (2.35 ± 0.08 kpc) of the nine earliest O-type stars are shown by horizontal dashed lines and blue wash. Mean distances and variances for Tr 16 (blue circle) and Tr 14 (red square) from Table 2 are shown along the left side. Several outliers with $S/N > 20$ could be foreground and background stars, and possibly escaping stars. These include three stars in Tr 14 (Tr 14-4 at 2.62 kpc, Tr 14-5 at 2.83 kpc, HD 303312 at 2.12 kpc) and HD 305518 at 2.00 kpc (in Col 228). However, none of these stars has an aberrant proper motion relative to cluster mean values.

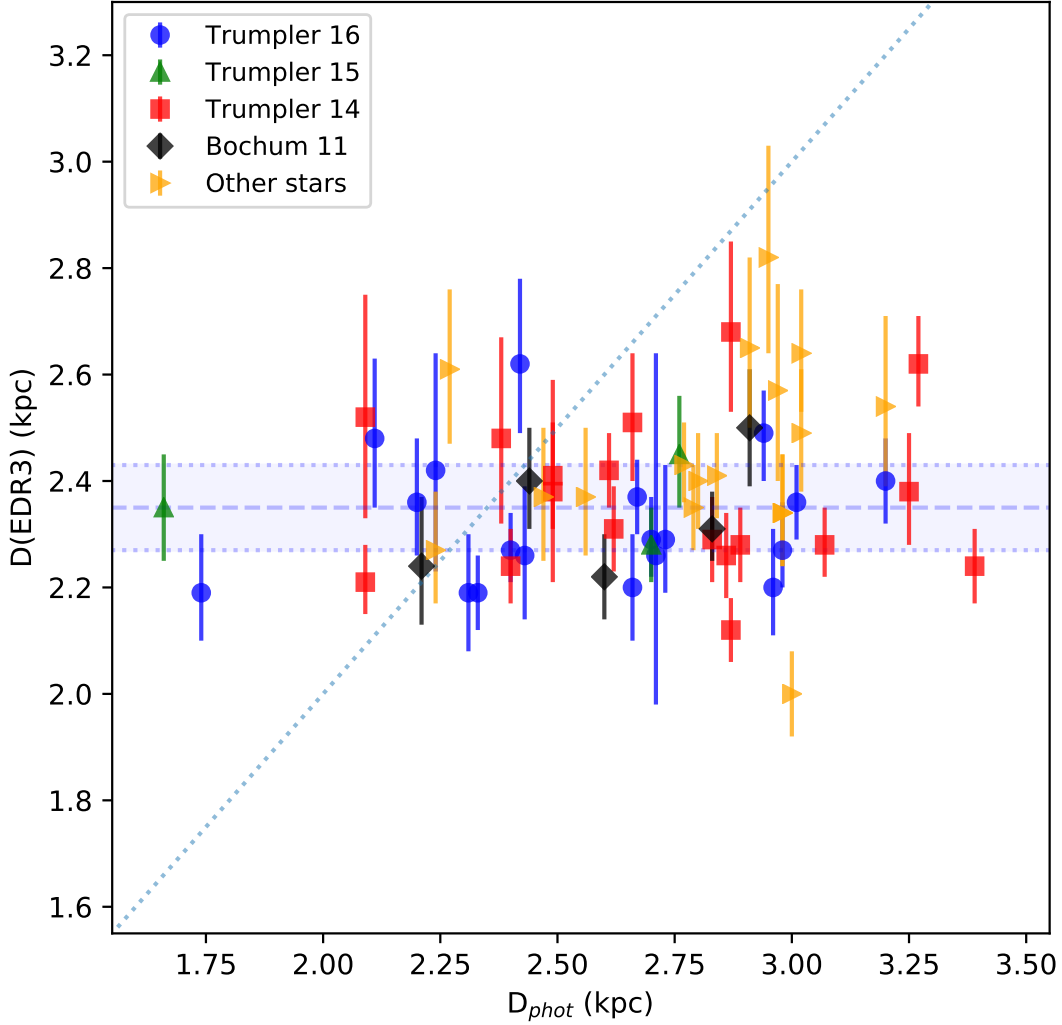


Fig. 2.— Comparison of Gaia-EDR3 distance with spectrophotometric distances in Table 2, color-coded for four clusters (Tr 16, Tr 15, Tr 14, Bo 11) and other stars. Horizontal lines and blue wash show the mean distance and rms variance to Car OB1, $D_{\text{EDR3}} = 2.35 \pm 0.08$ kpc. Two stars (Tr 14-5 and HD 93146B) with large, but uncertain values $D_{\text{phot}} > 4$ kpc, are not shown. HD 93146A has a realistic photometric distance, $D_{\text{phot}} = 2.30$ kpc, differing from that of HD 93146B. Using the M_V scale of Martins et al. (2005) would bring these distances into somewhat better agreement, still with some anomalies (see Tables 2 and 3).

Table 1. Previous Distance Estimates^a

Paper Name	Trumpler 14 <i>D</i> (kpc)	Trumpler 16 <i>D</i> (kpc)	Notes ^b
Thé & Vleeming (1971)	2.0 ± 0.2	2.5 ± 0.2	$R_V = 3.0$
Thé et al. (1980)	2.8 (2.3)	2.8 (2.4)	$R_V = 3.3$ (4.0)
Walborn (1973a)	3.5	2.6	UBV
Feinstein et al. (1973)	2.65 ± 10%	2.65 ± 10%	UBV ($R_V = 4.0$)
Humphreys (1978)	3.60 ± 0.15	2.69 ± 0.15	Blue/Red Supergiants
Turner & Moffat (1980)	2.70 ± 0.17	2.70 ± 0.17	UBV ($R_V = 3.20 ± 0.28$)
Thé et al. (1980)	2.3 ± 0.3	2.4 ± 0.3	UBV ($R = 4$)
Levato & Malaroda (1981)	...	2.6	V (Col 228) ($R_V = 3.2-4.0$)
Walborn (1982b)	2.8	2.8	UBV ($R_V = 3.0$)
Tapia et al. (1988)	2.4 ± 0.2	2.4 ± 0.2	JHKL
Morrell et al. (1988)	2.8 (3.45)	...	V; R_V variable (3.2)
Massey & Johnson (1993)	3.2 ± 4%	3.2 ± 4%	UBV ($R_V = 3.2$)
Allen & Hiller (1993)	...	2.2 ± 0.2	η Car expansion
Walborn (1982b)	2.8	2.8	UBV ($R_V = 3.0$)
Vázquez et al. (1996)	3.2 ± 10%	...	UBVRI
Davidson & Humphreys (1997)	...	2.3 ± 0.2	η Car
Meaburn (1999)	...	2.3 ± 0.3	η Car expansion
Davidson et al. (2001)	...	2.25 ± 0.18	η Car expansion
DeGioia-Eastwood et al. (2001)	3.6 ± 5%	3.61 ± 5%	UBV
Tapia et al. (2003)	2.8 ± 0.2	2.5 ± 0.2	UBVRIJHK
Carraro et al. (2004)	2.5 ± 0.3	4.0 ± 0.5	UBVRI
Smith (2006a)	...	2.35 ± 0.05	η Car expansion
Hur et al. (2012)	2.9 ± 0.3	2.9 ± 0.3	UBVI
Davidson et al. (2018)	3.0 ± 0.2	2.6 ± 0.2	Gaia-DR2
Kuhn et al. (2019)	2.64 ^{+0.31} _{-0.25}	2.61 ^{+0.31} _{-0.25}	Gaia-DR2
Povich et al. (2019)	2.50 ^{+0.28} _{-0.23}	2.50 ^{+0.28} _{-0.23}	Gaia-DR2

^aPhotometric distance estimates were estimated with various assumptions about the ratio of total-to-selective extinction, $R_V = A_V/E(B - V)$. These extinction corrections to *V* magnitudes provided distance moduli $DM = V - M_V - A_V$, typically ranging from 11.8 to 13.0 and converted to physical distances by the relation $D_{\text{phot}} = (10 \text{ pc})10^{DM/5}$.

^bNotes on photometry methods and assumed values of R_V (between 3.0 and 4.2). In a review, Walborn (2012) estimated a Tr 16 distance of (2.25 kpc)(0.8)^($R_V - 4$).

Table 2. Gaia Parallaxes and Distances^a

Star Name	Other	SpT	EDR3 ($\varpi \pm \sigma_\varpi$) (mas)	Offset (mas)	PM (mas/yr)	D_{EDR3} (kpc)	D_{phot} (kpc)	Notes (see text)
Trumpler 16:								
HD 93204 (#44)	Tr 16-178	O5.5 V	0.4240 ± 0.0226	0.012	7.524 ± 0.025	2.29[2.19,2.43]	2.73/2.40	
HD 93205 (#45)	V560 Car	O3.5 V	0.4308 ± 0.0248	0.012	8.169 ± 0.028	2.26[2.14,2.39]	2.43/2.34	+O8 V
HD 93250 (#48)	Tr 16-101	O4 III	0.4115 ± 0.0199	0.012	7.754 ± 0.023	2.36[2.26,2.48]	2.20/1.99	
HD 303308 (#137)	Tr 16-7	O4.5 V	0.4432 ± 0.0213	0.012	7.033 ± 0.023	2.20[2.10,2.30]	2.66/2.40	
CPD-59°2600 (#3)	Tr 16-100	O6 V	0.3914 ± 0.0226	0.012	7.362 ± 0.026	2.48[2.35,2.63]	2.11/1.86	
CPD-59°2603 (#4)	V572 Car	O7.5 V	0.3690 ± 0.0207	0.012	7.529 ± 0.024	2.62[2.49,2.78]	2.42/2.14	3, +B0 V
CPD-59°2591	Tr 16-21	O8.5 V	0.4056 ± 0.0131	0.017	7.178 ± 0.016	2.37[2.30,2.44]	2.67/2.37	
CPD-59°2624	Tr 16-9	O9.7 IV	0.4302 ± 0.0631	0.012	7.274 ± 0.079	2.26[1.98,2.64]	2.71/2.61	1, 3 (not 2634)
CPD-59°2626	Tr 16-23	O7.5 V	0.4009 ± 0.0346	0.013	7.768 ± 0.041	2.42[2.23,2.64]	2.24/1.98	
CPD-59°2627	Tr 16-3	O9.5 V	0.3904 ± 0.0136	0.012	7.397 ± 0.016	2.49[2.40,2.57]	2.94/2.62	
CPD-59°2628	V573 Car	O9.5 V	0.4428 ± 0.0200	0.011	7.537 ± 0.022	2.20[2.11,2.31]	2.96/2.64	+B0.5 V
CPD-59°2629	Tr 16-22	O8.5 V	0.4259 ± 0.0134	0.014	7.145 ± 0.016	2.27[2.21,2.34]	2.40/2.13	
V662 Car		O5 V	0.4126 ± 0.0127	0.011	7.195 ± 0.014	2.36[2.29,2.43]	3.01/2.64	+ B0 V
CPD-59°2635	Tr 16-34	O8 V	0.5171 ± 0.0186	0.012	7.258 ± 0.021	1.89[1.82,1.96]	2.50/2.23	+O9.5 V
CPD-59°2636AB	Tr 16-110	O8 V	not available	not available	2.34/2.08	3, +O8 V
CPD-59°2641	Tr 16-112	O6 V	0.4445 ± 0.0145	0.012	7.522 ± 0.017	2.19[2.12,2.26]	2.33/2.05	
CPD-59°2644	Tr 16-115	O9 V	0.4286 ± 0.0157	0.011	7.258 ± 0.018	2.27[2.20,2.36]	2.98/2.66	
HD 303316		O7 V	0.4241 ± 0.0138	0.012	6.732 ± 0.016	2.29[2.22,2.37]	2.70/2.39	
ALS 15210	Tr 16-244	O3.5 If*	0.4008 ± 0.0141	0.016	7.760 ± 0.016	2.40[2.32,2.48]	2.48/2.53	
HD 93162	WR25	O2.5 If*	0.4450 ± 0.0203	0.011	7.450 ± 0.023	2.19[2.10,2.30]	1.74/1.35	WN6+OB
HD 93343		O8 V	0.4452 ± 0.0228	0.012	7.338 ± 0.018	2.19[2.08,2.30]	2.31/2.05	
Mean values^b					7.417 ± 0.327	2.32 ± 0.12	2.56/2.31	
Trumpler 14:								
HD 93129A (#42)		O2 I	0.4037 ± 0.0175	0.012	6.874 ± 0.019	2.41[2.31,2.51]	2.49	3, AaAb
HD 93129B		O3.5 V	0.4073 ± 0.0162	0.012	6.969 ± 0.020	2.38[2.30,2.48]	2.49	3
HD 93128		O3.5 V	0.4256 ± 0.0150	0.012	6.952 ± 0.016	2.29[2.21,2.37]	2.83/2.73	
HD 93160		O7 III	0.3845 ± 0.0323	0.012	7.062 ± 0.034	2.52[2.33,2.75]	2.09/1.94	
HD 93161A	Tr 14-176	O7.5 V	0.3399 ± 0.0281	0.012	6.842 ± 0.029	2.84[2.69,3.09]	2.28/2.04	3, +O9 V
HD 93161B	Tr 14-176	O6.5 IV	0.3859 ± 0.0282	0.017	7.137 ± 0.029	2.48[2.32,2.67]	2.41/2.18	3
HD 303311		O6 V	0.4343 ± 0.0142	0.012	6.550 ± 0.016	2.24[2.17,2.31]	3.39/2.95	3
HD 303312	V725 Car	O9.7 IV	0.4599 ± 0.0138	0.012	6.819 ± 0.015	2.12[2.06,2.18]	2.87/2.76	
CPD-58°2611	Tr 14-20	O6 V	0.4263 ± 0.0127	0.012	6.992 ± 0.014	2.28[2.22,2.35]	3.07/2.70	
CPD-58°2620	Tr 14-8	O7 V	0.3610 ± 0.0217	0.012	7.172 ± 0.024	2.68[2.53,2.85]	2.87/2.54	
CPD-58°2627		O9.5 V	0.4027 ± 0.0182	0.017	6.986 ± 0.019	2.38[2.28,2.49]	3.25/2.90	
Tr 14-3		B0.5 V	0.4018 ± 0.0115	0.012	6.765 ± 0.012	2.42[2.35,2.49]	2.61	2, 3
Tr 14-4		B0 V	0.3647 ± 0.0127	0.017	7.033 ± 0.015	2.62[2.54,2.71]	3.27	2, 3
Tr 14-5		O9 V	0.3272 ± 0.0154	0.026	6.995 ± 0.019	2.83[2.71,2.96]	4.06/3.61	2, 3
Tr 14-6		B1 V	0.4199 ± 0.0149	0.023	6.751 ± 0.017	2.26[2.18,2.34]	2.86	2, 3
Tr 14-9		O8.5 V	0.4359 ± 0.0134	0.011	6.835 ± 0.015	2.24[2.17,2.31]	2.40/2.13	
Tr 14-27		B1.5 V	0.4270 ± 0.0136	0.025	6.567 ± 0.015	2.21[2.15,2.28]	2.09	2, 3
ALS 15204		O7.5 V	0.4198 ± 0.0152	0.014	7.215 ± 0.016	2.31[2.23,2.39]	2.62/2.31	
ALS 15206	CPD-58°2625	O9.2 V	0.3854 ± 0.0190	0.013	6.863 ± 0.021	2.51[2.40,2.64]	2.66/2.37	
ALS 15207	Tr 14-21	O9 V	0.4270 ± 0.0130	0.012	7.507 ± 0.014	2.28[2.21,2.35]	2.89/2.58	
Mean values^b					6.944 ± 0.221	2.37 ± 0.15	2.71/2.47	

Table 2—Continued

Star Name	Other	SpT	EDR3 ($\varpi \pm \sigma_\varpi$) (mas)	Offset (mas)	PM (mas/yr)	D_{EDR3} (kpc)	D_{phot} (kpc)	Notes (see text)
Trumpler 15:								
HD 93249		O9 III	0.3966 ± 0.0176	0.012	6.343 ± 0.019	2.45[2.35,2.56]	2.76/2.70	+O3 III
HD 303304		O7 V	0.4270 ± 0.0137	0.012	7.063 ± 0.017	2.28[2.21,2.35]	2.70/2.39	2, 3
HD 93190		O9.7 V:	0.4141 ± 0.0179	0.012	6.915 ± 0.020	2.35[2.25,2.45]	1.66/1.54	2, 3
Mean values^b					6.774 ± 0.380	2.36 ± 0.09	$2.37/2.21$	
Bochum 11:								
HD 93576	Bo 11	O9.5 IV	0.3887 ± 0.0181	0.012	6.488 ± 0.020	2.50[2.39,2.61]	2.91/2.70	
HD 93632	Bo 11	O5 If	0.4049 ± 0.0168	0.012	6.723 ± 0.021	2.40[2.31,2.50]	2.44/2.49	
HD 305539	Bo 11	O8 V	0.4204 ± 0.0130	0.012	6.627 ± 0.014	2.31[2.25,2.38]	2.83/2.51	
HD 305612	Bo 11	O8 V	0.4390 ± 0.0158	0.012	6.511 ± 0.017	2.22[2.14,2.30]	2.60/2.30	
ALS 18083	Bo 11	O9.7 V	0.4334 ± 0.0237	0.013	6.609 ± 0.027	2.24[2.13,2.37]	2.21/2.05	
Mean values^b					6.592 ± 0.095	2.33 ± 0.12	$2.60/2.41$	
Other Stars:								
HD 93028 (#41)	Col 228	O9 IV	0.3771 ± 0.0275	0.012	6.651 ± 0.031	2.57[2.40,2.77]	2.97/2.74	
HD 93222 (#47)	Col 228	O7 III	0.4102 ± 0.0228	0.012	6.832 ± 0.025	2.37[2.25,2.50]	2.47/2.30	3
HD 93146A (#43)	Col 228	O7 V	0.3288 ± 0.0358	0.012	6.807 ± 0.040	2.93[2.66,3.28]	2.30/2.03	3
HD 93146B	Col 228	O9.7 IV	0.3937 ± 0.0179	0.011	7.058 ± 0.019	2.47[2.37,2.59]	4.29/4.13	3
HD 93206A (#46)	QZ Car	O9.7 Ib	0.7356 ± 0.1086	0.013	6.252 ± 0.125	1.34[1.17,1.56]	2.23/2.33	3, +O8 III
HD 93130	Col 228	O6.5 III	0.3710 ± 0.0212	0.012	7.215 ± 0.024	2.61[2.47,2.76]	2.27/2.09	
HD 93027	Col 228	O9.5 IV	0.3424 ± 0.0242	0.012	7.377 ± 0.030	2.82[2.64,3.03]	2.95/2.74	
CPD-59°2554	Col 228	O9.5 IV	0.3645 ± 0.0226	0.011	7.024 ± 0.025	2.66[2.51,2.83]	2.91/2.70	
CPD-59°2551	Col 228	O9 V	0.3901 ± 0.0184	0.011	6.999 ± 0.020	2.49[2.38,2.61]	3.02/2.70	
CPD-59°2610	Col 228	O8.5 V	0.4158 ± 0.0192	0.011	7.097 ± 0.023	2.34[2.24,2.45]	2.98/2.64	
CPD-59°2673	Col 228	O5.5 V	0.3657 ± 0.0162	0.013	6.743 ± 0.019	2.64[2.53,2.76]	3.02/2.65	
HD 305438	Col 228	O8 V	0.3820 ± 0.0252	0.012	8.195 ± 0.030	2.54[2.39,2.71]	3.20/2.84	
HD 305518	Col 228	O9.7 III	0.4885 ± 0.0196	0.012	7.273 ± 0.021	2.00[1.92,2.08]	3.00/3.05	
HD 305523	Col 228	O9 II-III	0.4099 ± 0.0214	0.012	6.194 ± 0.025	2.37[2.26,2.50]	2.56/2.47	
HD 305524	Col 228	O6.5 V	0.4055 ± 0.0152	0.012	7.623 ± 0.017	2.40[2.31,2.49]	2.80/2.46	
HD 305532	TrC	O6.5 V	0.4031 ± 0.0142	0.012	7.070 ± 0.016	2.41[2.33,2.49]	2.84/2.50	
CPD-59°2661	TrC	O9.5 V	0.3992 ± 0.0145	0.026	7.017 ± 0.017	2.35[2.27,2.43]	2.79/2.49	
HD 305536	Col 228	O9.5 V	0.4296 ± 0.0206	0.011	7.275 ± 0.023	2.27[2.17,2.38]	2.24/2.00	
HD 305619	Col 228	O9.7 II	0.3992 ± 0.0120	0.012	7.208 ± 0.014	2.43[2.36,2.51]	2.77/2.61	
CPD-59°2610	Col 228	O8.5 V	0.4158 ± 0.0192	0.011	7.097 ± 0.023	2.34[2.24,2.45]	2.98/2.64	
Mean values^b					7.080 ± 0.207	2.45 ± 0.18	$2.75/2.53$	

^aParallax measurements for 68 OB stars in Carina OB1 association, including associated clusters (Trumpler 14, Trumpler 15, Trumpler 16, Collinder 228, Bochum 11, and Treasure Chest). Column 1 gives star name, with internal ID for 11 stars in the Shull & Danforth (2019) survey. Column 2 gives other names or cluster membership. Column 3 gives the SpT from GOSS except for seven stars. Column 4 lists parallaxes and errors from Gaia-EDR3. Column 5 gives the DR3 parallax offset (Lindgren et al. 2021) used for distance D_{EDR3} (and 1σ range) in column 7. Column 6 is the total proper motion (PM). Column 8 gives two photometric distances, based on GOSS photometry and SpTs when available, and absolute magnitudes M_V from Bowen et al. (2008) and Martins et al. (2005) respectively. Column 9 provides notes on binary companions and also: (1) GOSS typo in the identification of CPD-59°2624; (2) seven stars not found in GOSS; (3) methods for deriving photometric distances (see Appendix A).

^bMean EDR3 distances and (rms) variances of distance distributions were computed, omitting six stars with uncertain or missing data: two each in Tr 14, Tr 16, and Col 228 (see Section 2). Mean values for proper motion also omitted discrepant outliers (see Section 3). The mean photometric distances are 10–14% higher: 2.56 ± 0.28 kpc (Tr 16); 2.71 ± 0.36 kpc (Tr 14); 2.37 ± 0.61 kpc (Tr 15); 2.60 ± 0.29 kpc (Bo 11); and 2.75 ± 0.33 kpc (Other Stars).

Table 3. Stellar Distance Data^a

SpT	Star Name	ΔM_V (mag)	$D_{\text{phot}}^{(1)}$ (kpc)	$D_{\text{phot}}^{(2)}$ (kpc)	D_{EDR3} (kpc)
O3.5 V	HD 93205	0.08	2.43	2.34	2.26(2.14,2.39)
O3.5 V	HD 93128	0.08	2.83	2.73	2.29(2.21,2.37)
O4.5 V	HD 303308	0.22	2.66	2.40	2.20(2.10,2.30)
O5 V	V662 Car	0.29	3.01	2.64	2.36(2.29,2.43)
O5.5 V	HD 93204	0.28	2.73	2.40	2.29(2.19,2.43)
O5.5 V	CPD-59°2673	0.28	3.02	2.65	2.64(2.53,2.76)
O6 V	CPD-59°2600	0.28	2.11	1.86	2.48(2.35,2.63)
O6 V	CPD-59°2641	0.28	2.33	2.05	2.19(2.12,2.26)
O6 V	CPD-58°2611	0.28	3.07	2.70	2.28(2.22,2.35)
O6 V	HD 303311	0.28	3.39	2.99	2.24(2.17,2.31)
O6.5 V	HD 305524	0.28	2.80	2.46	2.40(2.31,2.49)
O6.5 V	HD 305532	0.28	2.84	2.50	2.41(2.33,2.49)
O7 V	HD 303316A	0.27	2.70	2.39	2.29(2.22,2.37)
O7 V	CPD-58°2620	0.27	2.87	2.54	2.68(2.53,2.85)
O7.5 V	CPD-59°2603	0.27	2.42	2.14	2.62(2.49,2.78)
O7.5 V	CPD-59°2626	0.27	2.24	1.98	2.42(2.23,2.64)
O7.5 V	ALS 15204	0.27	2.62	2.31	2.31(2.23,2.39)
O8 V	HD 93343	0.26	2.31	2.05	2.19(2.08,2.30)
O8 V	HD 305539	0.26	2.83	2.51	2.31(2.25,2.38)
O8 V	HD 305612	0.26	2.60	2.30	2.22(2.14,2.30)
O8 V	HD 305438	0.26	3.20	2.84	2.54(2.39,2.71)
O8.5 V	CPD-59°2591	0.26	2.67	2.37	2.37(2.30,2.44)
O8.5 V	CPD-59°2629	0.26	2.40	2.13	2.27(2.21,2.34)
O8.5 V	Tr 14-9	0.26	2.40	2.13	2.24(2.17,2.31)
O8.5 V	CPD-59°2610	0.26	2.98	2.64	2.34(2.24,2.45)
O9 V	CPD-59°2644	0.25	2.98	2.66	2.27(2.20,2.36)
O9 V	ALS 15207	0.25	2.89	2.58	2.28(2.21,2.35)
O9 V	CPD-59°2551	0.25	3.02	2.70	2.49(2.38,2.61)
O9.2 V	ALS 15206	0.25	2.66	2.37	2.51(2.40,2.64)
O9.5 V	CPD-59°2627	0.25	2.94	2.62	2.49(2.40,2.57)
O9.5 V	CPD-59°2628	0.25	2.96	2.64	2.20(2.11,2.31)
O9.5 V	CPD-58°2627	0.25	3.25	2.90	2.38(2.28,2.49)
O9.5 V	HD 305536	0.25	2.24	2.00	2.27(2.17,2.38)
O9.7 V	ALS 18083	0.16	2.21	2.05	2.24(2.13,2.37)
B0 V	Tr 14-4		3.27		2.62(2.54,2.71)
B0.5 V	Tr 14-3		2.61		2.42(2.35,2.49)
B1 V	Tr 14-6		2.86		2.26(2.18,2.34)
B1.5 V	Tr 14-27		2.09		2.21(2.15,2.28)

^aSpectrophotometric and parallax distances for 39 main-sequence stars in Car OB1 from O3.5 V to B1.5 V. There were no O4 V stars in the sample. $D_{\text{phot}}^{(1)}$ and $D_{\text{phot}}^{(2)}$ correspond to absolute magnitudes M_V from Bowen et al. (2008) and Martins et al. (2005), respectively, and all with GOSS photometry and SpTs. Columns 1 and 2 give the SpT and star name. Column 3 gives the difference ΔM_V in absolute magnitudes (the Martins magnitudes are fainter, but none were provided for B-type stars). The Gaia-EDR3 distances D_{EDR3} and range ($D_{\text{min}}, D_{\text{max}}$) are based on offset-corrected parallaxes and 1σ errors.

Table 4. Gaia Proper Motions^a

Star Name	PM _{RA} ^(Sun) (mas/yr)	PM _{Dec} ^(Sun) (mas/yr)	PM _{RA} ^(Car) (mas/yr)	PM _{Dec} ^(Car) (mas/yr)	PM _{tot} ^(Car) (mas/yr)	V _{tran} (km/s)
Trumpler 14:						
HD 93129A	-6.277 ± 0.019	2.801 ± 0.019	+0.303	+0.616	0.686 ± 0.082	7.64 ± 0.91
HD 93129B	-6.618 ± 0.020	2.182 ± 0.019	-0.038	-0.003	0.038 ± 0.063	0.42 ± 0.70
HD 93128	-6.616 ± 0.016	2.135 ± 0.016	-0.036	-0.050	0.062 ± 0.078	0.69 ± 0.87
HD 93160	-6.389 ± 0.034	3.011 ± 0.034	+0.191	+0.826	0.848 ± 0.090	9.45 ± 1.00
HD 93161A	-6.509 ± 0.029	2.109 ± 0.029	+0.071	-0.076	0.104 ± 0.079	1.16 ± 0.88
HD 93161B	-6.890 ± 0.029	1.862 ± 0.030	-0.310	-0.323	0.448 ± 0.079	4.99 ± 0.89
HD 303311	-6.213 ± 0.016	2.074 ± 0.016	+0.367	-0.111	0.383 ± 0.065	3.27 ± 0.72
HD 303312	-6.511 ± 0.015	2.025 ± 0.015	+0.069	-0.160	0.174 ± 0.082	1.94 ± 0.92
CPD-58°2611	-6.747 ± 0.014	1.837 ± 0.014	-0.167	-0.348	0.386 ± 0.081	4.30 ± 0.01
CPD-58°2620	-6.981 ± 0.024	1.642 ± 0.023	-0.401	-0.543	0.675 ± 0.080	7.52 ± 0.89
CPD-58°2627	-6.483 ± 0.019	2.603 ± 0.019	+0.097	+0.418	0.429 ± 0.085	4.78 ± 0.95
Tr 14-3	-6.450 ± 0.012	2.039 ± 0.014	+0.130	-0.146	0.195 ± 0.076	2.17 ± 0.84
Tr 14-4	-6.704 ± 0.015	2.126 ± 0.014	-0.124	-0.059	0.137 ± 0.067	1.53 ± 0.75
Tr 14-5	-6.619 ± 0.019	2.261 ± 0.016	-0.039	+0.076	0.085 ± 0.082	0.95 ± 0.91
Tr 14-6	-6.444 ± 0.017	2.014 ± 0.015	+0.136	-0.171	0.218 ± 0.077	2.43 ± 0.86
Tr 14-9	-6.486 ± 0.015	2.156 ± 0.014	+0.094	-0.029	0.098 ± 0.064	1.09 ± 0.72
Tr 14-27	-6.298 ± 0.015	1.859 ± 0.017	+0.282	-0.326	0.431 ± 0.076	4.80 ± 0.85
ALS 15204	-6.702 ± 0.016	2.670 ± 0.016	-0.122	+0.485	0.500 ± 0.083	5.57 ± 0.92
ALS 15206	-6.369 ± 0.021	2.557 ± 0.021	+0.211	+0.372	0.428 ± 0.082	4.77 ± 0.91
ALS 15207	-7.302 ± 0.014	1.741 ± 0.014	-0.722	-0.444	0.848 ± 0.069	9.45 ± 0.77
Mean values	-6.580 ± 0.060	2.185 ± 0.084			0.359 ± 0.058	4.00 ± 0.65
Trumpler 16:						
HD 93204	-7.089 ± 0.025	2.523 ± 0.026	-0.158	-0.089	0.181 ± 0.067	2.02 ± 0.75
HD 93205	-7.619 ± 0.028	2.947 ± 0.027	-0.688	+0.335	0.765 ± 0.068	8.52 ± 0.76
HD 93250	-7.116 ± 0.023	3.081 ± 0.023	-0.185	+0.469	0.504 ± 0.063	5.61 ± 0.70
HD 303308	-6.642 ± 0.023	2.313 ± 0.023	+0.289	-0.299	0.416 ± 0.065	5.12 ± 0.72
CPD-59°2600	-6.970 ± 0.026	2.368 ± 0.026	-0.039	-0.244	0.247 ± 0.064	2.75 ± 0.71
CPD-59°2603	-6.971 ± 0.024	2.844 ± 0.023	-0.040	+0.232	0.235 ± 0.063	2.62 ± 0.70
CPD-59°2591	-6.707 ± 0.016	2.559 ± 0.016	-0.224	-0.053	0.230 ± 0.065	2.56 ± 0.72
CPD-59°2624	-6.900 ± 0.079	2.302 ± 0.076	+0.031	-0.310	0.312 ± 0.096	3.48 ± 1.06
CPD-59°2626	-7.304 ± 0.041	2.645 ± 0.038	-0.373	+0.033	0.374 ± 0.075	4.17 ± 0.84
CPD-59°2627	-6.939 ± 0.016	2.564 ± 0.016	-0.008	-0.048	0.049 ± 0.060	0.55 ± 0.67
CPD-59°2628	-6.998 ± 0.021	2.799 ± 0.025	-0.067	+0.187	0.199 ± 0.063	2.22 ± 0.71
CPD-59°2629	-6.527 ± 0.016	2.906 ± 0.014	+0.404	+0.294	0.500 ± 0.063	5.57 ± 0.70
V662 Car	-6.724 ± 0.014	2.561 ± 0.013	+0.207	-0.051	0.213 ± 0.064	2.31 ± 0.71
CPD-59°2635	-6.783 ± 0.021	2.582 ± 0.019	+0.148	-0.030	0.151 ± 0.067	1.68 ± 0.75
CPD-59°2641	-7.015 ± 0.017	2.713 ± 0.015	-0.084	+0.101	0.131 ± 0.062	1.46 ± 0.69
CPD-59°2644	-6.799 ± 0.018	2.541 ± 0.017	+0.132	-0.071	0.150 ± 0.064	1.67 ± 0.72
HD 303316	-6.401 ± 0.016	2.083 ± 0.016	+0.530	-0.529	0.749 ± 0.063	8.34 ± 0.70
ALS 15210	-7.226 ± 0.016	2.828 ± 0.016	-0.295	+0.216	0.366 ± 0.063	4.08 ± 0.71
HD 93162	-6.918 ± 0.023	2.764 ± 0.023	+0.013	+0.152	0.153 ± 0.062	1.70 ± 0.69
HD 93343	-6.965 ± 0.018	2.311 ± 0.016	-0.034	-0.301	0.303 ± 0.060	3.38 ± 0.67
Mean values	-6.931 ± 0.063	2.612 ± 0.058			0.311 ± 0.044	3.46 ± 0.49
Bochum 11:						
HD 93576	-6.183 ± 0.020	1.967 ± 0.018	+0.130	+0.071	0.148 ± 0.042	1.65 ± 0.47
HD 93632	-6.442 ± 0.021	1.923 ± 0.021	-0.129	+0.027	0.132 ± 0.049	1.47 ± 0.55
HD 305539	-6.363 ± 0.014	1.853 ± 0.014	-0.050	-0.043	0.066 ± 0.041	0.74 ± 0.45
HD 305612	-6.251 ± 0.017	1.824 ± 0.018	+0.062	-0.072	0.095 ± 0.039	1.06 ± 0.44
ALS 18083	-6.325 ± 0.027	1.915 ± 0.029	-0.012	+0.019	0.022 ± 0.044	0.25 ± 0.49
Mean values	-6.313 ± 0.045	1.896 ± 0.026			0.093 ± 0.023	1.04 ± 0.25

^aProper motion components (mas/yr) in RA and Dec, in solar frame (columns 2 and 3) and Carina frame (columns 4 and 5) after subtracting mean values for each cluster (boldface). Errors on the mean, σ/\sqrt{N} , are derived from sample variance σ and number N in each cluster. Column 6 gives total parallax in cluster frame, from $PM_{\text{tot}}^2 = PM_{\text{RA}}^2 + PM_{\text{Dec}}^2$. Column 7 gives the star's transverse velocity (1 mas/yr is 11.14 km s⁻¹ at 2.35 kpc).